Korean J. Chem. Eng., 40(12), 2929-2940 (2023)
DOI: 10.1007/s11814-023-1487-y

pISSN: 0256-1115
eISSN: 1975-7220

Polymeric membranes for the oxygen enrichment of air in sulfur recovery units: Prevention of catalyst deactivation through BTX reduction

Seyed Heydar Rajaee Shooshtari†, Kiarash Bastani, and Hamidreza Eslampanah

Department of Chemical Engineering, Faculty of Engineering, Ferdowsi University of Mashhad, Mashhad, Iran
(*Received 29 September 2022 • Revised 6 April 2023 • Accepted 1 May 2023*)

Abstract−The modified Claus process is one of the most commonly used methods for hydrogen sulfide conversion into sulfur. However, one of the problems of this unit is the presence of benzene, toluene, and xylene (BTX) compounds at the inlet of the catalytic reactors that can deactivate the catalyst and decrease the efficiency of the sulfur recovery unit. One of the methods of BTX destruction in a furnace is to increase its temperature by increasing the oxygen concentration in the inlet air. In the present work, the application of polymeric membranes for the destruction of BTX was investigated by modeling and simulating a sulfur recovery unit and a membrane unit. The numerical results obtained from the simulations were validated successfully with industrial and experimental data for both sulfur recovery and membrane units. The simulation results for an industrial case study indicate that using five PI carbon membrane units with a total area of 26.82 m^2 can increase the concentration of oxygen in the inlet air to a level of 60%. In this condition, the reduction in BTX compounds can also be increased up to 59%. Furthermore, for two-stage membrane configuration, by employing five two-stage membrane units with a total area of 58.3 m^2, the oxygen concentration increases to 82%, and the reduction in BTX compounds will be 75%.

Keywords: Polymeric Membrane, Oxygen Enrichment, Modified Claus Process, BTX, Process Modeling

INTRODUCTION

Acid gas containing H_2S and CO_2 may naturally exist in natural gas at different concentrations. Furthermore, acid gas may form as a byproduct during desulfurization processes in oil and gas industries and also may be found in biogas from landfill waste [1,2]. H_2S is a very toxic and dangerous gas. It can be converted into SO_2 by combustion and cause acidic rain and significant damage to the environment [3]. Therefore, sulfur removal is one of the protocols of the Environmental Protection Agency (EPA) [4]. Governmental agencies worldwide have forced all their oil and gas industries to reduce sulfur emissions to the environment and protect it [5].

The sweetening process is commonly used in refineries to remove hydrogen sulfide from natural gas [6]. The sulfur recovery unit (SRU) that works on the modified Claus process is one of the most commonly used methods for converting H_2S to sulfur [7,8]. According to current environmental regulations, sulfur recovery efficiencies (SRE) must be higher than 99%. However, the efficiency of most SRUs that operate based on the modified Claus method is less than this value [9]. Therefore, improving the SRE of an SRU to the standard level is a very important issue, due to economic and environmental benefits [10].

In 1993, Khudenko et al. [11] suggested solutions for improving the SRE, such as using two furnaces in series or parallel, oxygen enrichment, and using an oxygen-air-water oxidizer. ZareNezhad [12] studied the effects of the pore size, the area, the particle size, and the shape of the catalyst on the performance of SRU. Several works [4,13-15] were focused on the maximization of sulfur production by finding the optimal values of the operating parameters of SRU, such as furnace pressure, furnace feed temperature, waste heat boiler (WHB) outlet temperature, and air and fuel flow to the furnace.

Ibrahim et al. [16] simulated the furnace kinetically and found that decreasing the furnace temperature from 1,105 °C to 1,050 °C reduces CO_2 emission by 60% and increases SRE by 0.2%. Ghahraloud et al. [17] showed that substituting adiabatic reactors with isothermal reactors in the catalytic section of SRU improves the efficiency of this unit. Rahman et al. [18] simultaneously minimized the energy consumption and emitted pollution from an SRU by considering the details of reaction mechanisms in the furnace.

Al Hamadi et al. [19] studied the effect of oxygen enrichment on the concentration of toluene, benzene, ethylbenzene, and xylene (BTEX) and toxic gas emissions, but did not mention the mechanism of oxygen enrichment. Also, some researchers focused on the effects of acid gas enrichment (AGE) and feed preheating on the furnace temperature and the destruction of BTEX and ammonia [5,8,9,20-22]. They concluded that AGE and feed preheating lead to a decrease in aromatic and ammonia content. Ibrahim [23] showed that temperature reduction of the first catalytic reactor would increase SRE, but this might decrease the hydrolysis of COS and CS_2. Abumounshar et al. [24] improved the performance of SRU for low H_2S content acid gases by using two combustion chambers and returning sulfur to the furnace.

There are various reasons for the Claus catalyst deactivation, which lead to a decrease in the SRU efficiency and high costs for catalyst regeneration or replacement. One of the most important reasons

†To whom correspondence should be addressed.
E-mail: rajaees@um.ac.ir

for SRU catalyst deactivation is the entering of BTEX into catalytic reactors. The destruction of BTEX before entering catalytic reactors by increasing the furnace temperature is the main solution to this problem. Enriching the air with oxygen is one of the ways to increase the furnace temperature and destroy BTEX before entering the catalytic section. The common processes for the oxygen-enrichment of air are pressure swing adsorption and cryogenic distillation, that are characterized by high energy consumption and high operating and investment costs [25,26]. The membrane separation process is one of the novel methods to enrich the air with oxygen. The advantages of this method over other methods are less energy consumption, lower capital and operational investment, and the possibility of utilization on a small and large scale, as well as simplicity of design [27].

Due to the attractive features of the polymeric membranes and for the first time, this study aimed to model and simulate an industrial membrane unit to enrich the air with oxygen at the entrance of the SRU furnace. For this purpose, first, the modeling and simulation of an industrial membrane unit and the simulation of SRU were carried out. After validating the results of both units with experimental and industrial data, the effects of oxygen enrichment on the furnace temperature, removal rate of BTX compounds, and improvement of SRU performance were investigated. Since different polymeric membranes with different properties (such as selectivity and permeance) can be used to separate oxygen from nitrogen, the performance of different polymeric membranes to enrich O_2 concentration in the air up to 60% was evaluated based on the required total surface area of each membrane and the number of membrane modules required in parallel. In this comparison, the temperature was fixed at 296.15 K, and the feed and permeate sides pressures were fixed at 100 bar and 1 bar, respectively. After choosing the best type of membrane, the suitable conditions for enriching the air with oxygen using single-stage membrane and two-stage membranes in series are discussed.

PROCESS MODELING AND SIMULATION APPROACH

As mentioned, this study is dedicated to the simultaneous modeling and simulation of membrane separation and sulfur recovery units to investigate the effect of oxygen enrichment at the inlet of the furnace on SRU performance. For this purpose, the membrane separation of oxygen from nitrogen is modeled. Then, the procedure of SRU simulation by ASPEN HYSYS V12 software is explained in detail.

1. Modeling of Oxygen Separation from Nitrogen by Polymeric Membranes

For the modeling and simulation of oxygen separation from nitrogen through polymeric membranes, a mathematical model based on total and partial mass balance equations along with pressure drop equation can be used on both feed and permeate sides [28]. A schematic of the countercurrent flow in a membrane for the separation of oxygen from nitrogen is shown in Fig. 1. As can be seen, the feed enters the shell side of the module with a specific flow rate and concentration. Furthermore, the membranes used here have higher permeability for oxygen, and the retentate stream is enriched with nitrogen.

In this modeling, the following assumptions are considered:

- The changes in the system properties, such as viscosity and permeance, are neglected.
- There is no mixing in the porous support layer.
- The high permeate flow rate prevents back diffusion.
- The feed side pressure drop is negligible.

Considering a differential permeator length dz along the membrane, mass balances of oxygen and nitrogen can be described as Eqs. (1) and (2), respectively [28,29]:

$$-\frac{d[Q_{FS}x_{FS}]}{dz} = J_{O_2}(\pi D_o N)(P_F x_{FS} - P_P x') \quad (1)$$

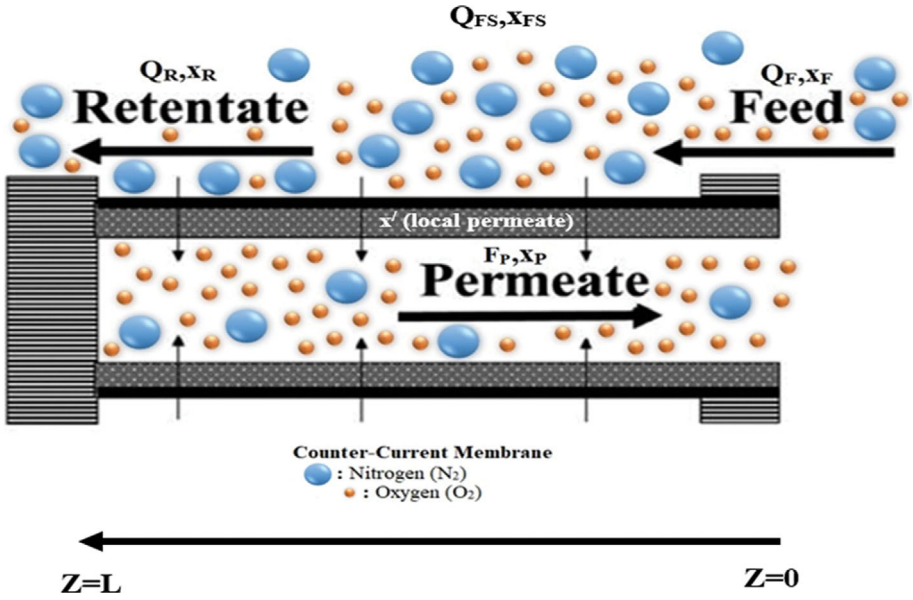

Fig. 1. Schematic diagram of shell-side feed countercurrent flow configuration.

$$-\frac{d[Q_{FS}(1-x_{FS})]}{dz}=J_{N_2}(\pi D_o N)(P_F(1-x_{FS})-P_P(1-x')) \quad (2)$$

where Q_{FS} is the flow rate at the feed side, x_{FS} is the mole fraction of oxygen at the feed side, J is the gas permeance, D_o is the outer diameter, N is the number of fibers, P_F is the feed side pressure, P_P is the permeate side pressure, and x′ is the local permeate mole fraction of oxygen.

The total mass balance over the differential permeator length dz can be expressed as Eq. (3) [28]:

$$\frac{dQ_{FS}}{dz}=\frac{dF_P}{dz} \quad (3)$$

where F_P is the flow rate at permeate side.

The differential equation for the feed side flow rate can be obtained by combining Eqs. (1) and (2), as below [28,29]:

$$\frac{dQ_{FS}}{dz}=-(\pi D_o N)[J_{O_2}(P_F x_{FS}-P_P x')+J_{N_2}(P_F(1-x_{FS})-P_P(1-x'))] \quad (4)$$

Additionally, the local permeate mole fraction is defined as Eq. (5), and the expansion of this equation can be written as Eq. (6) [28]:

$$x'=\frac{d(Q_{FS}x_{FS})}{dQ_{FS}} \quad (5)$$

$$x'=\frac{d(Q_{FS}x_{FS})}{dz}\times\frac{dz}{dQ_{FS}} \quad (6)$$

Substituting Eqs. (1) and (4) into Eq. (6) yields the following equation:

$$x'=\frac{J_{O_2}(\pi D_o N)(P_F x_{FS}-P_P x')}{(\pi D_o N)[J_{O_2}(P_F x_{FS}-P_P x')+J_{N_2}(P_F(1-x_{FS})-P_P(1-x'))]} \quad (7)$$

The membrane selectivity and pressure ratio are defined in Eqs. (8) and (9), respectively; and by substituting these equations into Eq. (7), the local permeate mole fraction can be simplified as Eq. (10).

$$\alpha=\frac{J_{O_2}}{J_{N_2}} \quad (8)$$

$$\delta=\frac{P_P}{P_F} \quad (9)$$

$$x'=\frac{\alpha(x_{FS}-\delta x')}{\alpha(x_{FS}-\delta x')+(1-x_{FS})-\delta(1-x')} \quad (10)$$

This equation is implicit with respect to x′. It can be rewritten as a second-order equation:

$$\delta(1-\alpha)x'^2+(1+(\alpha-1)(\delta+x_{FS}))x'-\alpha x_{FS}=0 \quad (11)$$

The physically acceptable solution of the above second-order equation is shown in Eq. (12):

$$x'=\frac{-(1+(\alpha-1)(\delta+x_{FS}))+\sqrt{(1+(\alpha-1)(\delta+x_{FS}))^2+4\delta(1-\alpha)(\alpha x_{FS})}}{2\delta(1-\alpha)} \quad (12)$$

Eq. (12) can be used to obtain the oxygen mole fraction between the feed and permeate sides (local permeate).

Furthermore, the combination of Eqs. (1) and (4) results in the differential equation of the oxygen mole fraction at the feed side (x_{FS}):

$$\frac{dx_{FS}}{dz}=-\frac{x_{FS}((\pi D_o N)[J_{O_2}(P_F x_{FS}-P_P x')+J_{N_2}(P_F(1-x_{FS})-P_P(1-x'))])}{Q_{FS}}-\frac{J_{O_2}(\pi D_o N)(P_F x_{FS}-P_P x')}{Q_{FS}} \quad (13)$$

As mentioned in the assumptions, the feed side pressure drop is negligible and the permeate side pressure drop can be estimated from the Hagen-Poiseuille equation [28,29]:

$$\frac{dP_P}{dz}=-\frac{128\mu RTF_P}{\pi D_i^4 N P_P} \quad (14)$$

where μ, R, T, and D_i are the gas viscosity, the universal gas constant, the temperature, and the inner diameter, respectively.

Eqs. (3), (4), (12), (13), and (14) can be solved simultaneously to obtain the values of molar flow rates at the feed and permeate sides, oxygen mole fraction at the feed side, permeate side pressure, and oxygen mole fraction between the feed side and permeate side along the membrane. Furthermore, in the countercurrent flow mode, the stage cut is defined as the ratio of the permeate flow rate to the feed flow rate at the feed inlet and permeate exit (z=0), as:

$$\vartheta=\left.\frac{F_P}{Q_{FS}}\right|_{z=0} \quad (15)$$

For the countercurrent flow configuration, the feed flow rate, composition and pressure are known at the feed inlet (z=0). However, the flow rate at the permeate side (F_P) should be selected via trial-and-error procedure to attain zero permeate flow rate at the permeate inlet (z=L). Therefore, after guessing an initial value for F_P, the local permeate mole fraction (x′) should be calculated from Eq. (12). Then, Eqs. (3), (4), (13), and (14) should be solved simultaneously to obtain the values of F_P, Q_{FS}, x_{FS} and P_P along the membrane length. If the permeate flow rate at the permeate inlet is not equal to zero, the steps should be repeated. The entire computational algorithm is shown in Fig. 2.

2. Methodology of Modeling and Simulation of SRU

2-1. Process Description

The main equipment of an SRU that works based on the modified Claus method includes a furnace, a WHB, heaters, catalytic beds, condensers, and an incinerator, as illustrated in Fig. 3 [30]. In the furnace of the Claus process, acid gas reacts with air and more than 1500 main and side reactions occur. The amount of air must be such that H_2S/SO_2 ratio is about two at the furnace outlet [20].

The furnace outlet stream enters WHB at a high temperature, wherein water evaporates and decreases the temperature of the furnace outlet stream. Note that the temperature drop in WHB changes the equilibrium conditions, and reactions proceed in WHB. After cooling the WHB outlet stream by the condenser, and separating liquefied sulfur, the gas stream enters a heater. The main reason for preheating this stream before entering catalytic reactors is to prevent capillary condensation of sulfur. Typically, the catalytic section consists of three reactors containing alumina catalysts.

Three main reactions occur in catalytic reactors: Claus reaction (Eq. (16)), hydrolysis of COS (Eq. (17)), and hydrolysis of CS_2 (Eq. (18)).

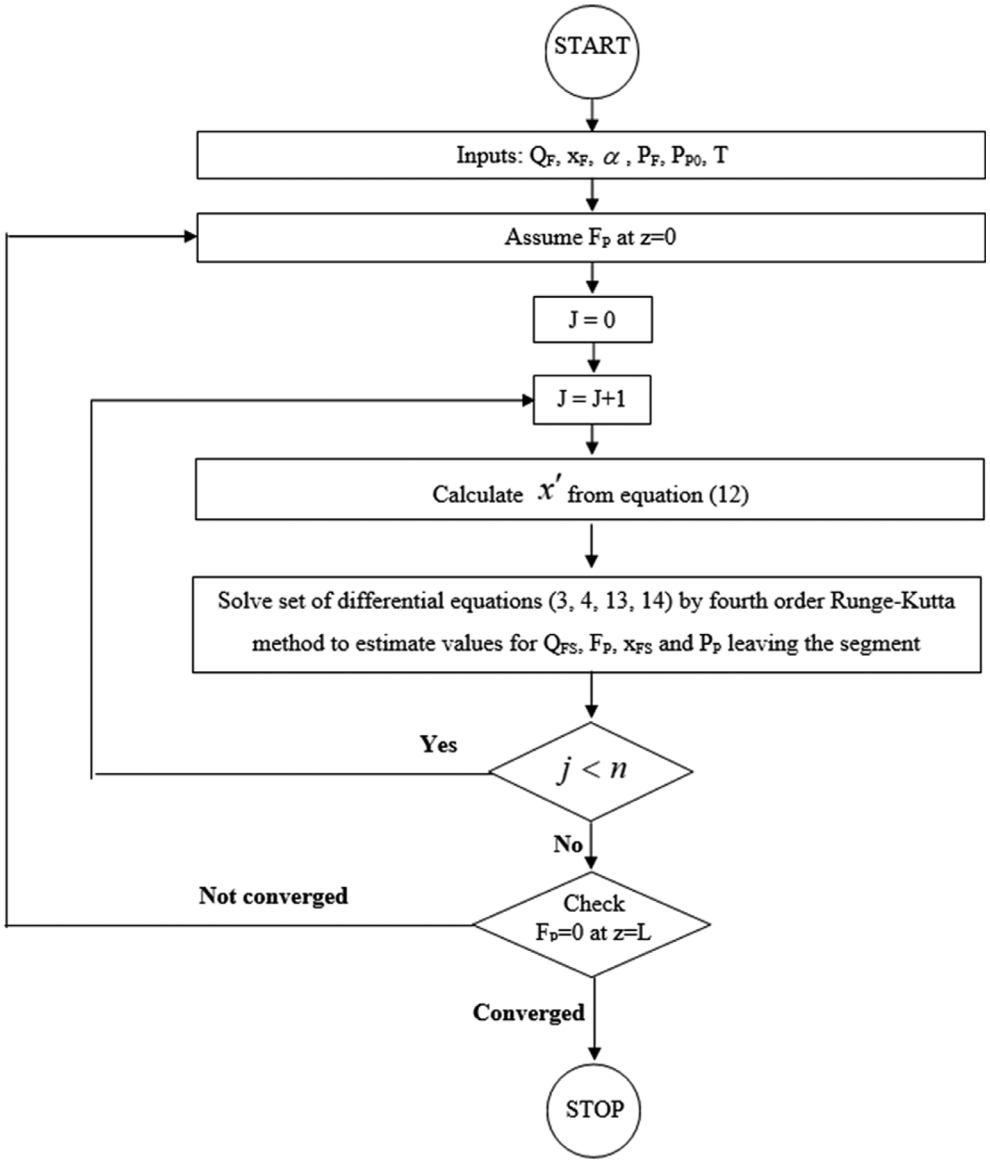

Fig. 2. Computational algorithm for simulation of countercurrent membrane used for oxygen enrichment.

$$H_2S+SO_2 \rightleftharpoons 3S+2H_2O \quad (16)$$

$$COS+H_2O \rightleftharpoons CO_2+H_2S \quad (17)$$

$$CS_2+2H_2O \rightleftharpoons CO_2+2H_2S \quad (18)$$

After each catalytic reactor, there is a condenser that condenses the produced sulfur from the reactor outlet stream. Eventually, the outlet stream from the catalytic stage enters an incinerator and unreacted H_2S is burned and converted into SO_2.

2-2. Process Modeling

In the present work, ASPEN HYSYS V12 is used to simulate an SRU based on the modified Claus method. The assumptions considered in this simulation are as follows:

- Steady-state conditions
- Equilibrium conditions in the furnace
- Adiabatic state in the furnace and catalytic sections

In ASPEN HYSYS software, the Claus process furnace is simulated based on the Gibbs free energy minimization method, which is an equilibrium approach. The advantage of this method is that there is no need to specify the reactions and their stoichiometry, and the results are in good agreement with actual data. The inlet air flow rate should be adjusted so that the ratio of H_2S to SO_2 becomes 2 at the furnace outlet stream. Furthermore, the WHB is modeled as a single-pass heat exchanger.

The ASPEN HYSYS software also considers the catalytic reactors in equilibrium conditions, and free energy minimization calculations are performed by the software, based on the inlet conditions and the outlet pressure. However, there is a parameter called approach to equilibrium (ATE) in the catalytic reactor section of the software that determines the progress of reaction to the equilibrium conditions, and is a criterion for the deactivation of catalysts. Since the rate of reaction progress directly affects the outlet temperature of reactors, the ATE parameter can be determined by trial and error if the outlet temperature of reactors is known.

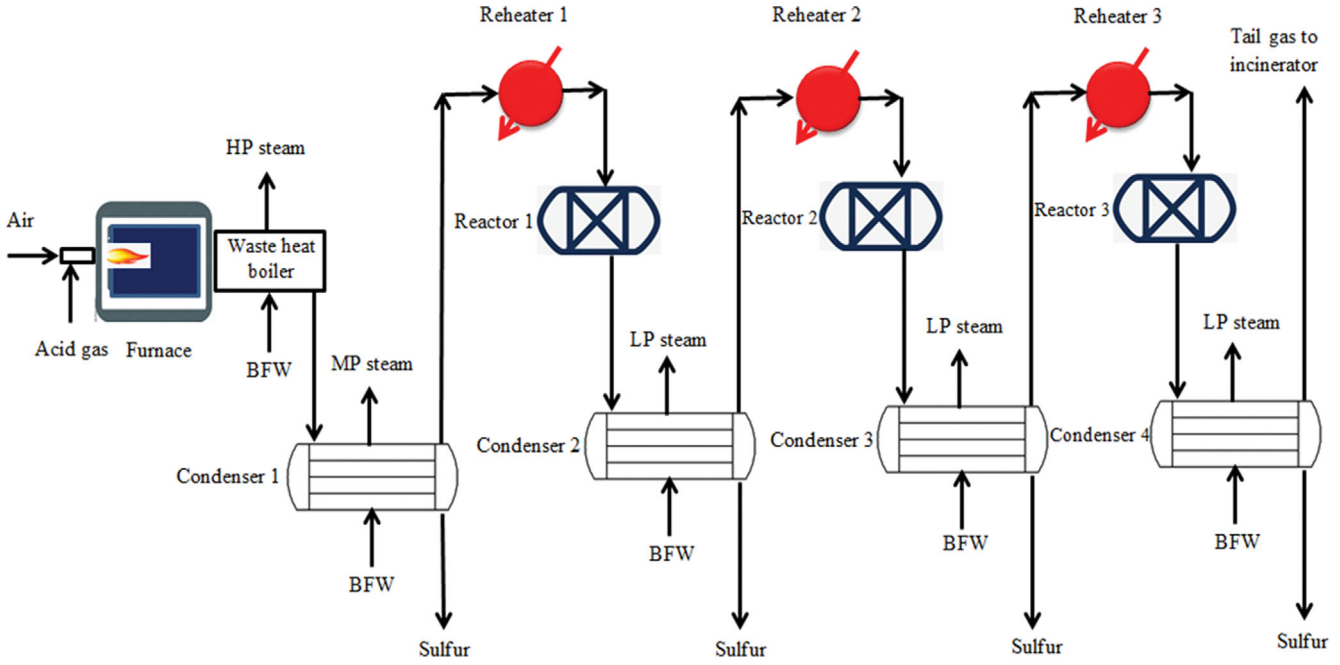

Fig. 3. Process flow diagram of SRU based on modified Claus method [30].

RESULTS AND DISCUSSION

As mentioned, this study focused on using membranes to improve SRU performance. In this section, first, the model presented in the previous section is validated. Then the performance of an industrial SRU is improved by oxygen enrichment using an industrial membrane module. Since no experimental data is available for the combination of these two units, each unit (SRU and membrane separation) is validated separately.

1. Membrane Unit Model Validation

The experimental data of Feng et al. [29] are used in this section to validate the presented model for oxygen separation from the air by hollow fiber asymmetric membrane based on cellulose acetate. The shell-side feed countercurrent flow configuration was used in their experimental data. The necessary data for validation of the suggested model is presented in Table 1.

Table 1. Operating conditions and membrane configuration for model validation [28,29]

Parameters	Unit	Value
Total fibers	-	368
Inner diameter	m	80×10^{-6}
Outer diameter	m	160×10^{-6}
length	m	0.25
Feed temperature	°C	23
Feed pressure	kPa	790.80
Permeate pressure	kPa	101.3
O_2 Permeance	mol/m^2·Pa·s	30.78×10^{-10}
N_2 Permeance	mol/m^2·Pa·s	5.7×10^{-10}
Feed composition		
O_2	mole percent	20.5
N_2	mole percent	79.5

In Fig. 4, the simulation results of the proposed model are compared with experimental data of Feng et al. [29]. For a better comparison, two statistical parameters, including the root mean square error (RMSE) and the coefficient of determination (R^2), are also included in Fig. 4. As seen in Fig. 4, the simulation results are in good agreement with experimental data.

2. SRU Simulation Validation

The complete simulation of SRU was done in ASPEN HYSYS

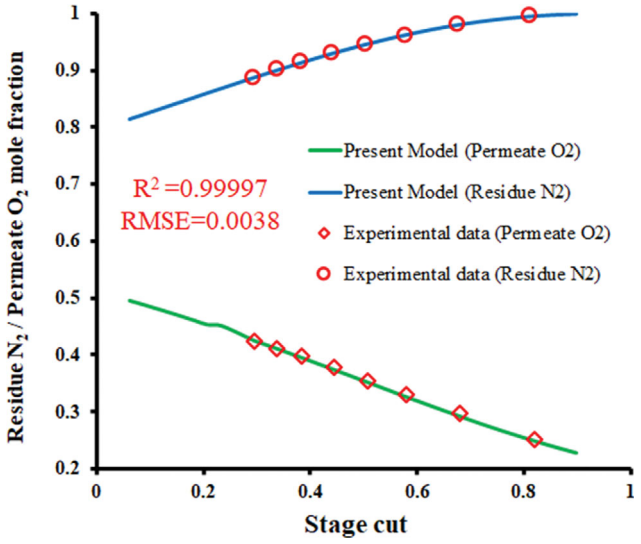

Fig. 4. Comparison between the proposed model predictions and experimental data of Feng et al. [29] for separation of O_2 from N_2.

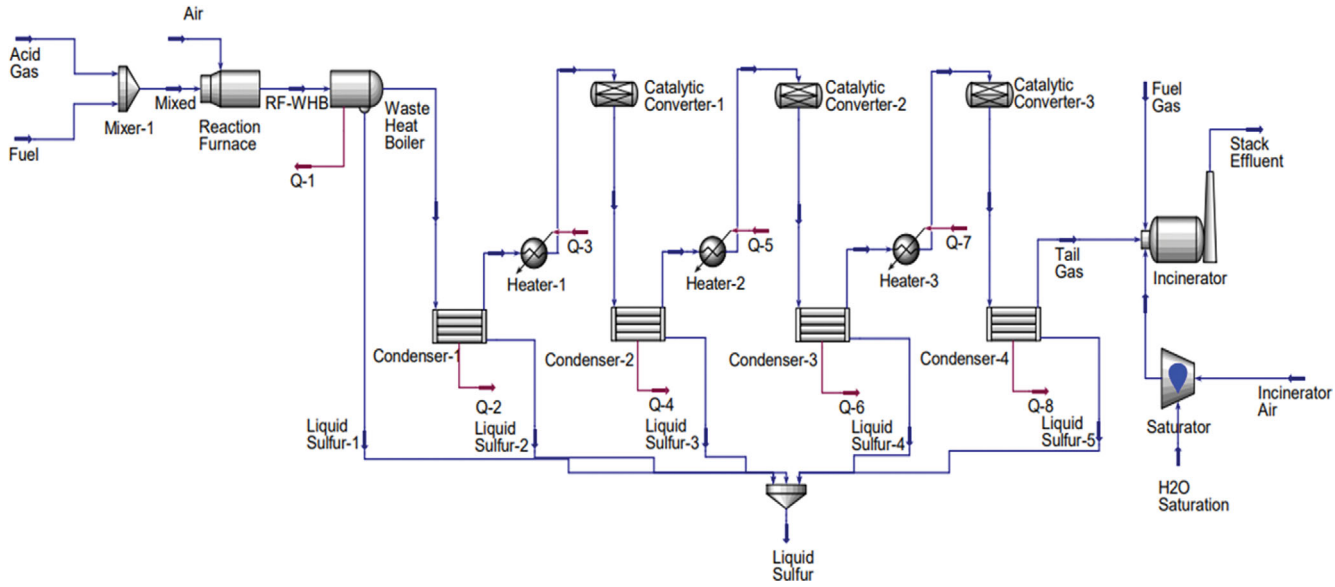

Fig. 5. General SRU schematic simulated in ASPEN HYSYS software.

Table 2. Inlet conditions and feed composition of South Pars SRU furnace [31]

	Unit	Acid gas	Air	Fuel gas
Temperature	K	491.15	493.15	313.15
Pressure	kPa	177	168	600
Feed components				
CO_2	mole percent	53.16	0	1.03
O_2	mole percent	0	19.5	0
N_2	mole percent	0	73	3.68
H_2S	mole percent	36.04	0	0
H_2O	mole percent	9.9	7.5	0
CH_4	mole percent	0.9	0	89.46
C_2H_6	mole percent	0	0	5.66
C_3H_8	mole percent	0	0	0.17
Total molar flow	mol/s	171.11	181.5	3.24
Furnace				
Residence time in furnace	s		2	

Table 3. Operating conditions of South Pars SRU catalytic section [31]

	Unit	First reactor	Second reactor	Third reactor
Inlet temperature	K	508.53	478.45	468.28
Outlet temperature	K	580.75	495.15	471.25
Inlet pressure	kPa	138	126	114
Outlet pressure	kPa	134	122	110

software. A schematic of this simulation is shown in Fig. 5.

Since this study aims to use membranes to improve SRU performance, it is essential to compare SRU simulation results with actual industrial data. The SRU data of South Pars Refinery [31] are used for this purpose. The required data for the thermal and catalytic sections are presented in Tables 2 and 3, respectively.

Fig. 6 compares the simulation results and the industrial data of the furnace and the first to the third catalytic reactors of South Pars SRU. Since the order of magnitude of species flow rates is in an extensive range, these diagrams are drawn in logarithmic scale to cover all data. Also, similar to Fig. 4, the root mean square error and the coefficient of determination are included in Fig. 6. As can be seen, the results of this simulation agree well with the industrial data of South Pars SRU.

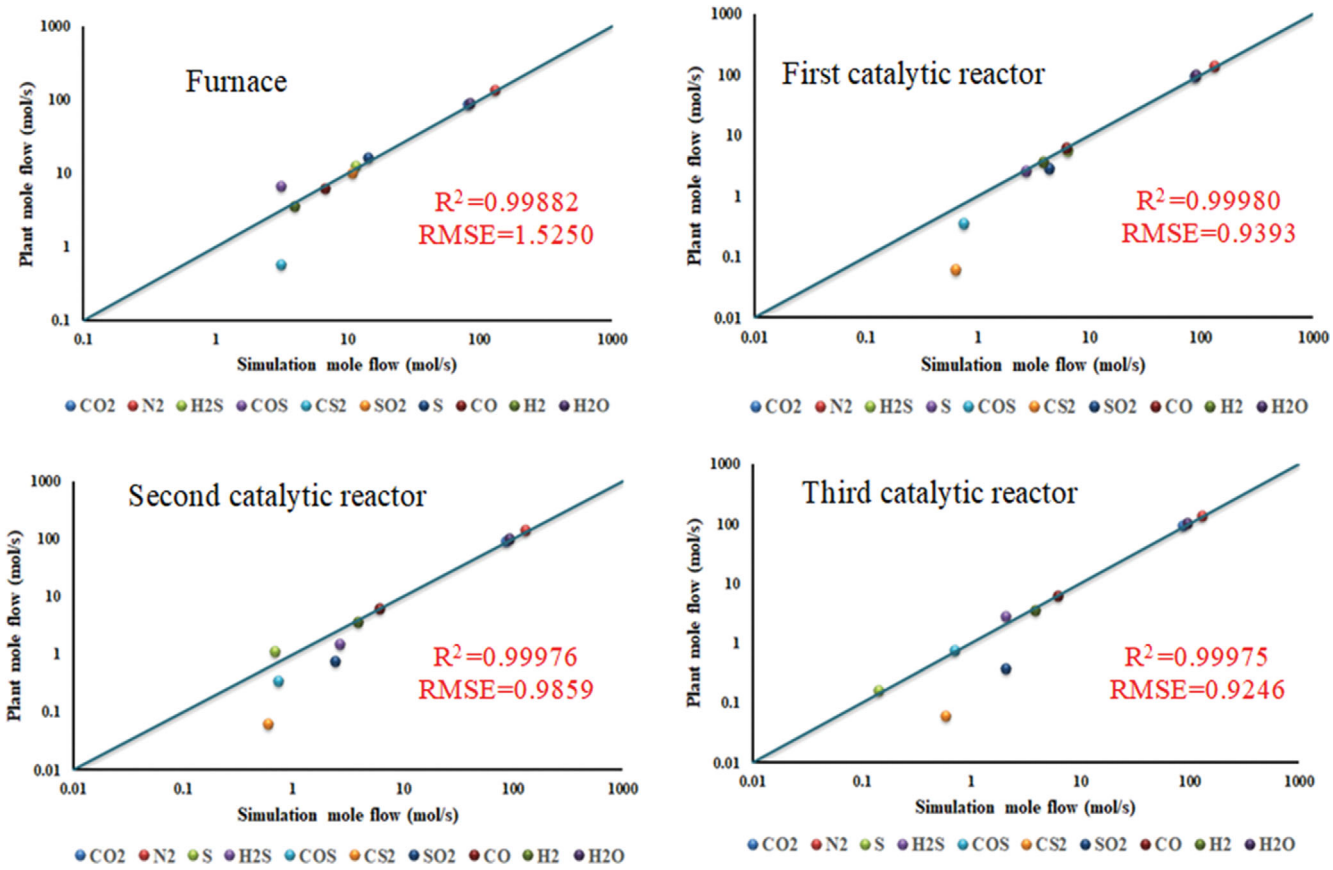

Fig. 6. Comparison between the simulation results and industrial data of South Pars SRU [31].

3. Simulation Results

Generally, the presence of BTX in the inlet feed is one of the problems of SRU. These compounds can deactivate SRU catalyst significantly. The catalyst deactivation not only decreases its lifetime but also can reduce SRE. Therefore, the reduction of BTX at the inlet stream of catalytic reactors is vital from an economic point of view and also increases sulfur production and reduces the emission of pollutants such as SO_2 to the environment.

3-1. Case Study Description

This investigation aims to enrich the air with oxygen using polymeric membranes to improve SRU performance through BTX destruction in the SRU furnace. This becomes even more important at furnaces with relatively low temperatures. For example, in the Khangiran natural gas refinery, the inlet acid gas to the unit is lean and the H_2S/CO_2 ratio is low. So, the maximum temperature of the furnace reaches 840 °C, which cannot destroy BTX. Therefore, suggesting solutions to increase the furnace temperature and, as a result, BTX destruction, is essential. One of the commonly used methods for increasing the furnace temperature is using co-firing. Although this method has many advantages, it also has some operational problems, such as increasing the required air flow rate, increasing fuel cost, higher CS_2 production in the furnace, unit capacity reduction, and the possibility of hydrocarbon escaping to other units. Another method of increasing the furnace temperature is the oxygen enrichment of inlet air through membranes, which is the focus of this investigation.

Therefore, although South Pars SRU data were used in the previous section to validate the simulation results, Khangiran natural gas refinery data are used here to investigate the effect of using membranes on the performance improvement of SRU. The reason for choosing this case study is the low temperature of its furnace, which causes no destruction of aromatic compounds in the furnace. The entry of these compounds into the catalyst beds is one of the most important causes of catalyst deactivation and reducing the efficiency of sulfur production in this refinery. Inlet acid gas conditions and composition of Khangiran natural gas refinery SRU are presented in Appendix A [32]. The inlet air flow rate is adjusted so that the ratio of H_2S to SO_2 will equal 2 at the furnace outlet stream.

3-2. The Effect of Oxygen Enrichment on the Performance of SRU

The effect of enriching the air with oxygen on furnace temperature, BTX reduction in the furnace outlet stream, and the required air are shown in Fig. 7. The model suggested by Flowers et al. [33] was used for the estimation of BTX reduction. They used experimental data to find a correlation between temperature and BTX reduction. They reported that BTX destruction starts at 900 °C and increases with increasing temperature. As can be seen in Fig. 7, by increasing the concentration of oxygen to 37%, the furnace temperature increases to 900 °C and BTX destruction begins. The reason is that the presence of nitrogen in inlet air disturbs the combustion reaction, and prevents the effective collision of the atoms in the main reactions in the furnace. By increasing oxygen concentration in the air, the combustion process takes place more effectively,

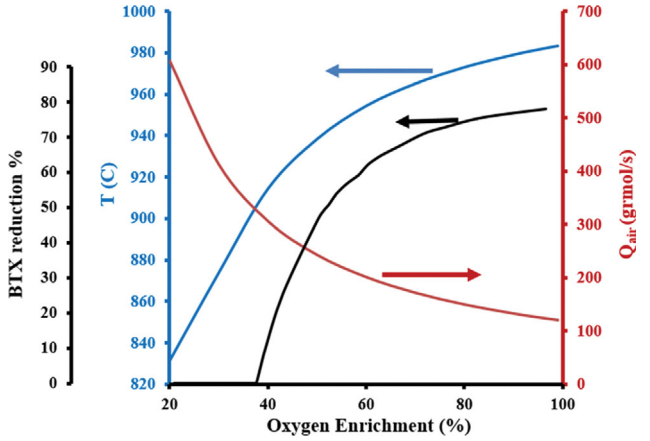

Fig. 7. Effects of oxygen enrichment on furnace temperature, BTX reduction, and required air flow rate.

which leads to increase in temperature of the furnace. Since BTX is destroyed at high temperatures, increasing the furnace temperature decreases BTX concentration in the furnace outlet stream.

Furthermore, Fig. 7 shows that increasing the oxygen concentration will decrease the required air to maintain the ratio of H_2S to SO_2 of 2 to 1 in the furnace outlet stream. The reason is that as the concentration of oxygen increases in the air, the share of oxygen in the furnace inlet air increases, which leads to better combustion of H_2S. The decrease in required inlet air not only increases the unit capacity, but also decreases the required steam at the inlet blowers of the unit, which is economically significant.

According to Fig. 7, it can be concluded that by increasing the oxygen concentration to about 60%, the amount of BTX decreases sharply. Afterward, the slope of the changes decreases. At this extent of oxygen enrichment, the reduction in BTX compounds increases to 59%. Furthermore, the furnace temperature and the required airflow rate reach about 954.4 °C and 200.6 mol/s, respectively.

3-3. The Effect of Membrane Type on the Oxygen Enrichment Process

Polymeric membranes can be utilized for the oxygen enrichment of air. Some examples of such membranes with their characteristics are listed in Appendix B. These membranes have different permeance and selectivity, which leads to their different performances in separating oxygen from nitrogen.

Table 4. Membrane configuration (geometry) and operating conditions for O_2 enrichment

Parameters	Unit	Value
Inner diameter	m	0.02
Outer diameter	m	0.064
Membrane length range	m	0.016-1
Number of fibers	-	1,800
Feed temperature	K	296.15
Feed pressure	bar	100
Permeate pressure	bar	1
Feed velocity	m/s	25

As illustrated in the previous section, the concentration of BTX compounds at the furnace outlet considerably decreases by enriching the air up to 60% of oxygen. For this reason, the effective membrane area for 60% enrichment of inlet air is considered for comparing the membranes presented in Appendix B. The industrial dimensions of membrane units used for oxygen enrichment from 20.5% to higher values are also presented in Table 4. Note that to reduce the number of required membrane units and the area of the membranes, the feed pressure of the membrane was set to 100 bar. Furthermore, the length of different membranes was determined based on the 60% oxygen mole percent in the outlet permeate stream.

The critical point is that the permeate flow rates are not the same for the different membranes. If the permeate flow rate is equal to the required airflow in Fig. 7, enrichment of the inlet air would be possible in just one stage. On the other hand, if the permeate flow rate is less than the required air, it is necessary to use some parallel membrane units to supply the required inlet air. The number of these units can be determined by dividing the required air to permeate flow rate according to Eq. (19):

$$N = \frac{Q_{air}}{F_P} \tag{19}$$

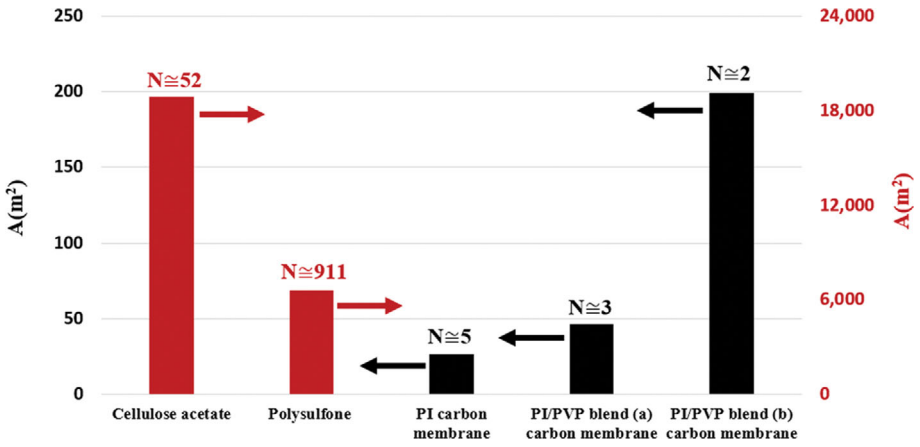

Fig. 8. Comparison of different membrane areas and required numbers for 60% oxygen enrichment.

The calculated number of stages and total area of different membranes to enrich the inlet air with 60% oxygen for Khangiran refinery SRU are compared in Fig. 8. As seen, the PI carbon membrane has a much better performance compared to other membranes in terms of the required area. Using this membrane, five parallel membrane units with a total area of 26.82 m^2 can enrich the inlet air with 60% oxygen. Therefore, the performance of this membrane in O_2/N_2 separation will be investigated in the next section, focusing on the distributions of the important parameters along the membrane.

3-4. Investigating the Distributions of Various Parameters along the PI Membrane Length

As illustrated in the previous section, the PI carbon membrane showed a better performance in the separation of oxygen from nitrogen. The oxygen mole fraction distribution on both sides of the PI carbon membrane is shown in Fig. 9. As the feed moves along the membrane, the oxygen mole fraction decreases in the retentate stream. The reason is a higher rate of oxygen diffusion compared to nitrogen due to its higher permeance. Furthermore, Fig. 9 indicates that the oxygen mole fraction decreases in both bulk and local permeate along the membrane length. The reason is that at Z=0, the inlet stream enters at the feed side with the maximum oxygen concentration. Since the streams are countercurrent, the stream exits at permeate side at Z=0. At this point, the feed stream has the maximum oxygen concentration, so both permeate and local permeate also have the maximum oxygen mole fraction. When the stream moves along the membrane on the feed side, the oxygen mole fraction decreases due to oxygen diffusion through the membrane and, as a result, the oxygen mole fraction decreases in both bulk and local permeate. Note that the oxygen local permeate mole

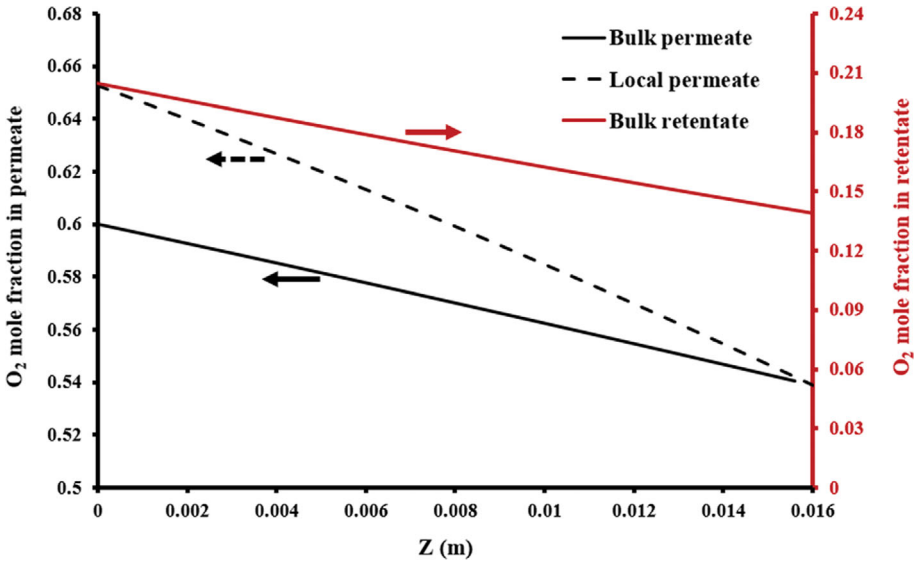

Fig. 9. Distributions of the O_2 mole fraction in the bulk permeate, the local permeate, and the bulk retentate along the membrane length.

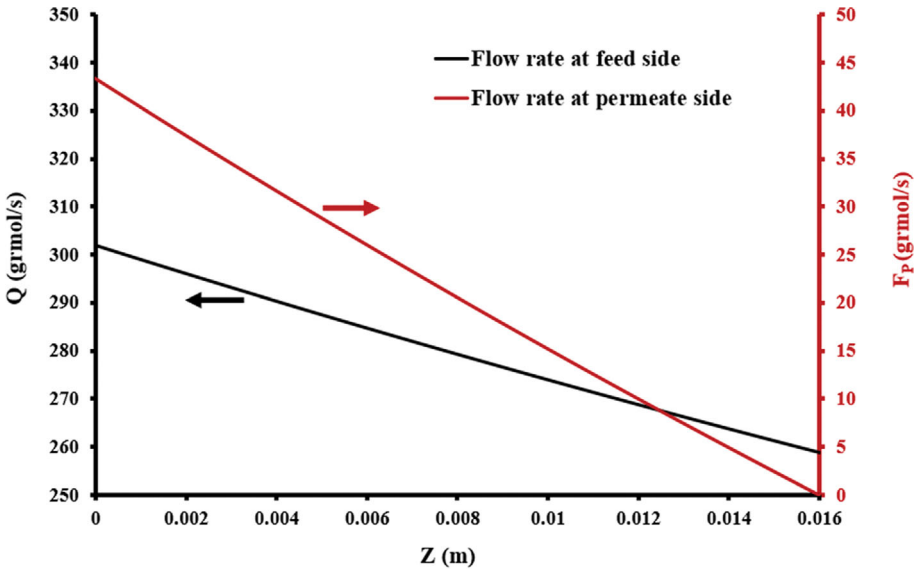

Fig. 10. Distributions of feed side and permeate side flow rates along the membrane length.

fraction is always higher than the oxygen mole fraction in the bulk permeate. This is because there is no stream in the local permeate, and the concentration in this section is related to the oxygen mole fraction in cavities that exist in the local permeate. However, there is fluid movement in the permeate side, and the concentration at each point of permeate side is affected by the concentration of previous points with lower oxygen mole fractions. Since at Z=0.016, the stream enters the permeate side of the membrane, and no stream exists before that, the oxygen concentration in both bulk permeate and local permeate is identical.

Fig. 10 illustrates the molar flow rates at the permeate and feed sides. As can be seen, as the feed stream on the feed side flows along the membrane length, its flow rate decreases due to oxygen diffusion to the permeate side. Since the streams flow in opposite directions and the permeate starts to flow at Z=0.016, its flow rate decreases along the membrane length to reach zero flow at the inlet of the permeate side. Therefore, the permeate flow rate and the oxygen concentration at the permeate side have their maximum values at Z=0, and can enter the Claus process furnace.

3-5. Two-Stage Membrane Separation Process

As seen in the previous section, using a one-stage PI carbon membrane, the oxygen concentration in the permeate stream reaches about 60%. To increase the oxygen concentration at the inlet of the Claus furnace, the first membrane permeate can be fed to another membrane module after increasing its pressure. The pressure increase between the two stages is economically significant and has considerable effects on the performance of a two-stage membrane unit. Fig. 11(a) presents the outlet oxygen mole fraction and the total area of the two-stage membrane unit versus the pressure between the two membranes. As can be seen, the oxygen mole fraction at the outlet stream of the second membrane decreases with increasing the inlet pressure. The reason for this is that with increasing pressure the nitrogen diffusion also increases, which leads to a decrease in the concentration of oxygen in the permeate side.

In addition, according to Fig. 11(a), increasing the inlet pressure of the second membrane decreases the total membrane area of the two stages, and it becomes constant at pressures higher than 40 bar. Based on Fig. 11(b), the reason for this observation is that increasing the pressure increases the flow rate at the permeate side (F_{P0}). On the other hand, since oxygen concentration decreases with increasing the pressure, the required air increases, according to Fig. 7. Based on Eq. (19), the number of required units (N) increases with increasing the required air flow rate, while increasing the permeate side flow rate has the opposite effect on the number of required units. As can be seen in Fig. 11(b), for pressures less than 40 bar, the effect of permeate side flow rate on the number of required units is greater, while for higher pressures, the increase in both required air and permeate side flow rates cancel each other's effect and N remains constant at pressures higher than 40 bar. So, the total membrane area also becomes constant at pressures higher than 40 bar.

Considering all the mentioned points, it can be concluded that the pressure increase to more than 40 bar does not have a positive effect on the second membrane performance, and 40 bar can be chosen as the optimum inlet pressure of the second membrane. So, for Khangiran natural gas refinery SRU, if five two-stage membrane modules with 58.3 m^2 total area are used and the pressure increases to 40 bars between the two stages, the oxygen enrichment will reach 82%. In this case, the temperature of the Claus process furnace will be about 974 °C, and BTX destruction reaches 75%.

As mentioned in the introduction, there are other methods for oxygen enrichment from air, such as cryogenic distillation and pressure swing adsorption. Cryogenic distillation is most commonly used for the separation of oxygen from air which can produce oxygen with purity of up to 99%. However, this method also has disadvantages, such as complexity of the procedure/process and high energy usage.

Using the PSA method, it is possible to produce oxygen with purity up to 95%. However, this method also has disadvantages, such as high operational and capital costs, high energy consumption, process complexity, and lack of flexibility. On the other hand, membrane separation has been proven to be a suitable process for oxygen enrichment because of its simple design, flexibility, ease of scaling up, ability to combine with other technologies, ease of installation, smaller footprint, less fuel, and electricity consumption and the presence of a wide variety of membranes with different permeability and selectivity [25,35].

Adhikari et al. [25] compared the cost of production of oxygen-enriched air using PSA, cryogenic distillation, and membrane processes. They reported that oxygen enrichment by the membrane has a lower production cost than PSA and is competitive with cryo-

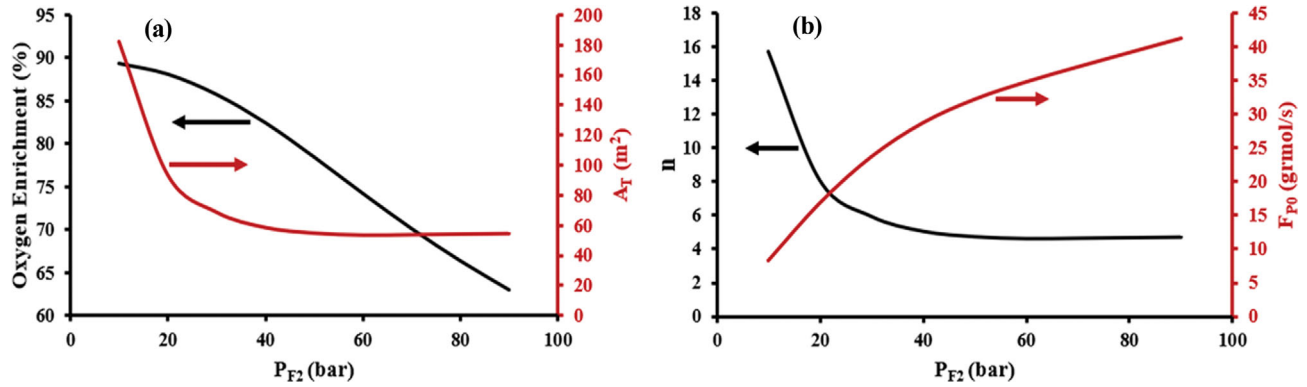

Fig. 11. Effects of the second stage inlet pressure on the: (a) Oxygen enrichment percent and total area, (b) Number of units and permeate outlet flow rate.

genic distillation. Furthermore, in another research, Valappil et al. [35] reported that producing oxygen-enriched air by polymeric membranes is an attractive and energy-efficient alternative for PSA and cryogenic distillation.

According to the above mentioned, the membrane separation system is a suitable and attractive method for air separation. For this reason, it was used in the present study to improve the performance of SRU. Finally, although installing a membrane system in the sulfur recovery unit requires investment costs, it can significantly reduce the cost of replacing the catalyst. Furthermore, preventing the deactivation of the catalyst can increase the efficiency of the unit and increase the sulfur production rate, which, in addition to being economical, is very important from an environmental point of view.

CONCLUSION

Considering the importance of eliminating BTX compounds in the furnace of the Claus process in SRU, the present study focused on designing, modeling and simulating an industrial membrane unit for enriching air with oxygen, increasing the furnace temperature, and destruction of BTX compounds. The destruction of BTX compounds in the furnace is important considering that the entry of these compounds into the catalyst beds can lead to the deactivation of the catalyst and ultimately reduce the efficiency of sulfur recovery. After validating the results obtained from the simulations of both membrane and sulfur recovery units, the effects of oxygen enrichment by membrane technology on the performance of SRU of Khangiran natural gas refinery were investigated, and the following results were obtained:

1. By using five parallel PI carbon membranes with a total area of 26.82 m^2, the oxygen concentration in the inlet air of the furnace increased to about 60%.

2. Increasing the oxygen concentration to 60% was found to increase the furnace temperature from 840 °C to 954.4 °C. In this condition, the reduction in BTX compounds increased to 59%, and the required air flow rate decreased from 607 mol/s to 200.6 mol/s.

3. In the case of using two-stage membrane-separation units, the optimum intermediate pressure between the two stages was determined as about 40 bar.

4. In the optimal conditions, using five two-stage membrane units with a total area of 58.3 m^2, the oxygen concentration, and the SRU furnace temperature increased up to 82% and 974 °C, respectively. Furthermore, the reduction in BTX compounds was about 75%, and the required air also decreased to 149 mol/s.

5. Reducing the concentration of BTX compounds at the outlet of the furnace can increase the lifetime of catalysts and lead to an increase in the efficiency of sulfur production. This issue is very important not only from an economic aspect but also environmentally.

REFERENCES

1. J. H. Yang, *Korean J. Chem. Eng.*, **38**(4), 674 (2021).
2. S. Ibrahim, R. K. Rahman and A. Raj, *Appl. Therm. Eng.*, **156**, 576 (2019).
3. E. Keshavarz, D. Toghraie and M. Haratian, *Appl. Therm. Eng.*, **123**, 277 (2017).
4. M. A. Zahid, M. Ahsan, I. Ahmad and M. N. Aslam Khan, *Mathematics*, **10**(1), 88 (2022).
5. R. K. Rahman, S. Ibrahim and A. Raj, *Chem. Eng. Sci.*, **155**, 348 (2016).
6. Y. Li, Q. Guo, Z. Dai, Y. Dong, G. Yu and F. Wang, *Appl. Therm. Eng.*, **117**, 659 (2017).
7. B. Mahmoodi, S. H. Hosseini, G. Ahmadi and A. Raj, *Appl. Therm. Eng.*, **123**, 699 (2017).
8. P. Abdoli, S. A. Hosseini and M. A. Mujeebu, *Forsch. Ingenieurwes*, **83**, 81 (2019).
9. S. Ibrahim, A. Jagannath and A. Raj, *J. Nat. Gas. Sci. Eng.*, **83**, 103581 (2020).
10. M. H. Ahmadi, M. Mehrpooya and F. Pourfayaz, *Appl. Therm. Eng.*, **109**, 640 (2016).
11. M. Khudenko, G. M. Hitman and T. E. P. Wechsler, *J. Environ. Eng.*, **119**(6), 1233 (1993).
12. B. ZareNezhad, *J. Ind. Eng. Chem.*, **15**(2), 143 (2009).
13. S. Zarei, H. Ganji, M. Sadi and M. Rashidzadeh, *Appl. Therm. Eng.*, **103**, 1095 (2016).
14. H. Ghahraloud, M. Farsi and M. R. Rahimpour, *J. Taiwan. Inst. Chem. Eng.*, **76**, 1 (2017).
15. H. Kazempour, F. Pourfayaz and M. Mehrpouya, *J. Nat. Gas. Sci. Eng.*, **38**, 235 (2017).
16. S. Ibrahim, R. K. Rahman and A. Raj, *Abu Dhabi International Petroleum Exhibition & Conference*, OnePetro (2018), https://doi.org/10.2118/192771-MS.
17. H. Ghahraloud, M. Farsi and M. R. Rahimpour, *Chem. Prod. Process. Model.*, **14**(2) (2019).
18. R. K. Rahman, S. Ibrahim and A. Raj, *Comput. Chem. Eng.*, **128**, 21 (2019).
19. M. Al Hamadi, S. Ibrahim and A. Raj, *Ind. Eng. Chem. Res.*, **58**(36), 16489 (2019).
20. B. ZareNezhad and N. Hosseinpour, *Appl. Therm. Eng.*, **28**, 738 (2008).
21. S. Ibrahim, R. K. Rahman and A. Raj, *Appl. Therm. Eng.*, **156**, 576 (2019).
22. S. Ibrahim, M. Al Hamadi and A. Raj, *Ind. Eng. Chem. Res.*, **59**(11), 4912 (2020).
23. A. Y. Ibrahim, *Pet. Petro. Chem. Eng J.*, **5**(1), 1 (2021).
24. N. Abumounshar, A Raj and S. Ibrahim, *Chem. Eng. Sci.*, **248**(B), 117194 (2022).
25. B. Adhikari, C. J. Orme, J. R. Klaehn and F. F. Stewart, *Sep. Purif. Technol.*, **268**, 118703 (2021).
26. I. S. Moon, D. I. Lee, J. H. Yang and H. W. Ryu, *Korean J. Chem. Eng.*, **3** (1), 15 (1986).
27. S. Haider, A. Lindbråthen, J. A. Lie and M. B. Hägg, *Sep. Purif. Technol.*, **205**, 251 (2018).
28. P. K. Kundu, A. Chakma and X. Feng, *Can. J. Chem. Eng.*, **99**(5), 1253 (2011).
29. X. Feng, J. Ivory and V. S. V. Rajan, *AIChE J.*, **45**(10), 2142 (1999).
30. S. Mokhatab, W. A. Poe and J. Y. Mak, Gulf Professional Publishing, 4th ed. (2018).
31. N. Javanmardi Nabikandi and S. Fatemi, *J. Ind. Eng. Chem.*, **30**, 50 (2015).

32. E. Kourosh and A. Shahsavand, *Nashrieh Shimi va Mohandesi Shimi Iran*, **33**, 99 (2014).
33. J. Flowers, T. Chow and V. Wong, *Sulphur*, **333**, 42 (2011).
34. M. Bozorg, B. Addis, V. Piccialli, Á. A. Ramírez-Santos, C. Castel, I. Pinnau and E. Favre, *Chem. Eng. Sci.*, **207**, 1196 (2019).
35. R. S. K. Valappil, N. Ghasem and M. Al-Marzouqi, *J. Ind. Eng. Chem.*, **98**, 103 (2021).

APPENDIX A. CASE STUDY INFORMATION

The inlet air consists of 20.89% O_2, 78.81 N_2, and about 0.3% H_2O. Furthermore, the inlet conditions and feed composition are illustrated in Table A1.

Table A1. Inlet conditions and feed composition of Khangiran natural gas refinery SRU [32]

Parameters	Unit	Acid gas
Temperature	K	325.15
Pressure	kPa	150.96
Feed components		
CO_2	mole percent	56.30
H_2S	mole percent	33.60
H_2O	mole percent	9.04
CH_4	mole percent	1.05
Benzene	ppm	59.26
Toluene	ppm	19.75
Xylene	ppm	8.20
Total molar flow	mol/s	745.3

APPENDIX B. MEMBRANES PROPERTIES FOR O_2/N_2 SEPARATION

The characteristics of different membranes used to enrich the inlet air with oxygen are shown in Table A2.

Table A2. Various membranes and their properties for O_2/N_2 separation [25,28,34]

Membrane	O_2 permeance ($mol/m^2 \cdot Pa \cdot s$)	O_2/N_2 selectivity
PI carbon membrane	2.72×10^{-6}	7.5
PI/PVP blend (a) carbon membrane	2.01×10^{-6}	10
PI/PVP blend (b) carbon membrane	6.70×10^{-7}	15
Cellulose acetate	30.78×10^{-10}	5.4
Polysulfone	9.045×10^{-9}	5.7